Natural Hazards **27:** 47–60, 2002.

Seismic Source Parameters for the $M_L = 5.4$ Athens Earthquake (7 September 1999) from a New Telemetric Broad Band Seismological Network in Greece

G. N. STAVRAKAKIS, G. CHOULIARAS and G. PANOPOULOU
Institute of Geodynamics, National Observatory of Athens, P.O. Box 20048, 118 10 Athens, Greece
E-mail: g.choul@egelados.gein.noa.gr

Received: 11 July 2000; accepted in revised form: 2 March 2001

Abstract. A regional telemetric network of twelve digital broad-band seismic stations has been in full operation since the beginning of 1999, in Greece, operated by the Institute of Geodynamics of the National Observatory of Athens (GI-NOA). On 7 September 1999, a $M_L = 5.4$ main shock occurred just 18 kilometers to the north of the Greek capital Athens, causing severe damage and loss of life. The broad band network recorded the seismic sequence and the main shock and 18 aftershocks were selected in order to determine their seismic source parameters and scaling relations by the spectral analysis method.

The results indicate a main shock seismic moment $M_0 = 5.7 \times 10^{24}$ dyn-cm in general agreement with that reported by other agencies and two different source models were used to determine the respective fault radii and displacements for comparison and evaluation purposes.

In addition, by investigating source parameters for the aftershocks, it was found that the seismic moment correlates very well with the earthquake magnitude (M_L) and corner frequency (F_C) through the following relationships: Log $M_0 = 1.80M_L + 15.19$ and Log $M_0 = -3.17F_C + 22.09$, respectively. These results and scaling relations are in general agreement with those obtained by other studies and in view of the fact that digital seismic instrumentation is now expanding in Greece, these first results from spectral analysis of digital broad band data can be considered useful for future relevant investigations.

Key words: Athens earthquake, spectral analysis, source parameters.

1. Introduction

The Greek National Seismographic network operated and maintained by GI-NOA is currently composed of 12 digital stations (Figure 1) and will in the near future be expanded to 20. Each station is equipped with a three component Lennartz LE-3d/20 second sensor, a Teledyne S-13 vertical component sensor, a Teledyne DR-24 digitizer with a sampling rate of 50 Hz and a GPS receiver. The data from the two horizontal broad band channels and the verical short period component are transmitted to the main data aquisition center in Athens by leased line telemetry, at a baud rate of 19200. The data aquisition system employs a newly developed soft-

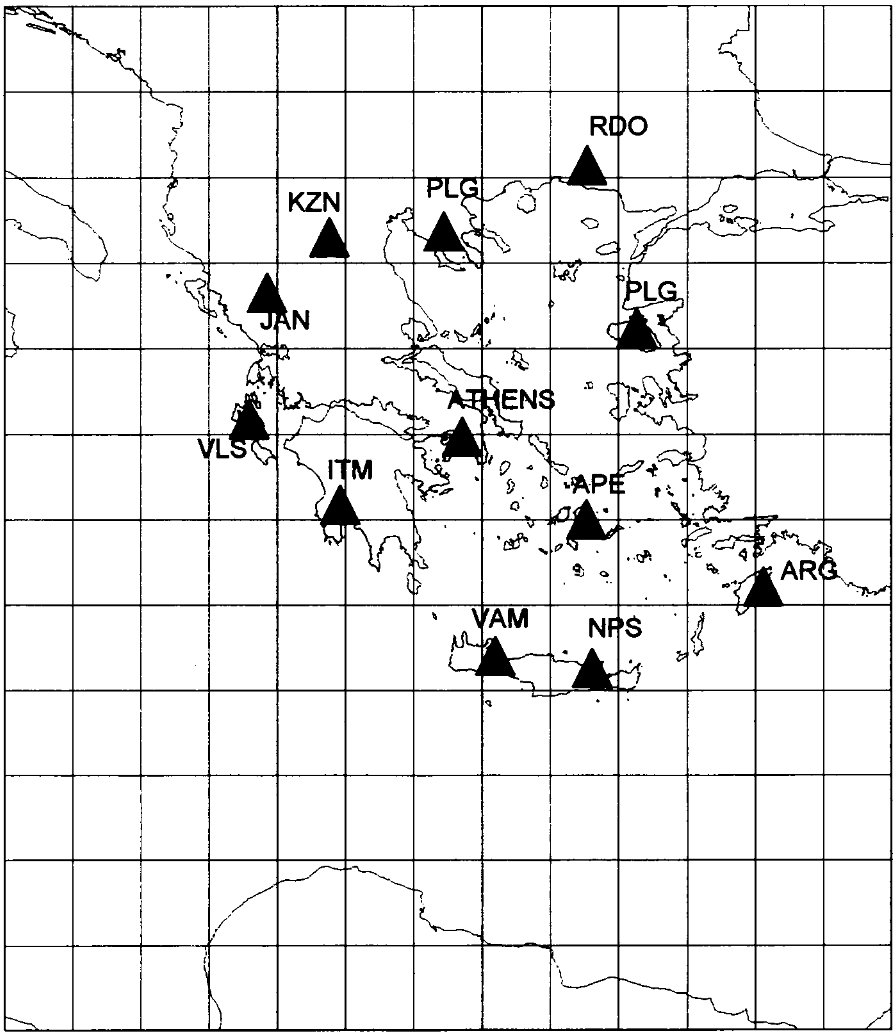

Figure 1. The digital broad-band network operated by GI-NOA.

ware configuration whereby an STA/LTA criterion is used to detect seismic events and archive the recorded waveforms. At the same time, an auto-pick algorithm provides a quick estimate of the epicenter and magnitude of a triggered event if the STA/LTA criterion is fulfilled at more than three stations.

This broad band network is part of the ORFEUS European broad band network configuration and in the near future the data will be available to the scientific community via Internet using the well known AUTODRM procedure.

On 7 September 1999 at 11:38 G.M.T an earthquake sequence begun 18 kilometers north of Athens with a magnitude M_L = 3.2 event, followed by 2 other smaller shocks at 11:40 and 11:43 G.M.T both with M_L = 2.5. The main shock of the sequence occurred a few minutes later at 11:56 G.M.T with a magnitude

M_L = 5.4 that devestated the city of Athens, causing extensive damage to the buildings in the north and western parts of the city, with a human toll of roughly 100,000 homeless and 143 deaths. The mostly damaged area was located in the northwestern suburbs of the city and in total 100 buildings collapsed and 13,000 were considered beyond repair. The horizontal peak ground acceleration values for the main shock mainly ranged between 0.075 and 0.50 g with the value of 0.31 g being indicated as the most representative by Papadopoulos *et al.* (2000).

Ambraseys (1994) after a thorough investigation concludes that "The historical seismicity record of Athens appears to have been almost free of destructive earthquakes" and a map of the nearby historical events from that study is shown in Figure 2. In addition to that, the recent seismic history of the area since 1900 as revealed by the earthquakes catalogs of Makropoulos *et al.* (1989) from 1900–1963 and the earthquake catalog of NOA from 1964–1999, as seen in Figure 3, does not indicate any previous significant seismic activity in the specific area where the main shock was located.

Immediately after the event, GI-NOA installed an array of 40 portable digital and analog stations in the vicinity of the main shock in order to monitor the aftershock activity. The spatial distribution of epicenters as determined Stavrakakis *et al.* (1999), can be seen in Figure 4a and one clearly sees a WNW-ESE trend in the epicentral distribution, which is in good agreement with the determined fault plane solutions by Louvari and Kiratzi (2000), Papadopoulos *et al.* (2000) and Tselentis and Zahradnic (2000) and also with geologic and seismotectonic field investigations by Pavlides *et al.* (1999, 2000) which indicates that the seismogenetic structure consists of a normal fault striking 110°–130°N and dipping 50°–80°SW.

The moment tensor solution for the main shock as determined by the U.S.G.S, indicates a fault azimuth of 123°, a dip of 55°, a seismic moment of 7.8 $\times 10^{24}$ dyn cm with M_W = 5.9, while the Harvard CMT solution gives approximately similar results, with an azimuth of 114°, a dip of 47° and a seismic moment of 1.15 $\times 10^{25}$ dyn cm with M_B = 5.8.

The results of the present study concerning the seismic moment and fault dimensions of the main shock and 18 of the largest aftershocks, are found to be in good agreement with other relevant investigations and results.

2. Data and Analysis

The digital broad band data from the GI-NOA seismographic network were used to determine the earthquake source parameters and scaling relations, of the main shock and of 18 well recorded aftershocks, with magnitudes greater than $M_L = 3.5$, by the spectral analysis method.

The earthquakes used in this study are listed in Table 1, together with their parameters as listed in the GI-NOA bulletins. The coordinates of the main shock are the relocated ones as described in Papadopoulos *et al.* (2000) and focal mechanisms were determined in the same study for events 1, 7, 8, 10, 11, 14–19 on

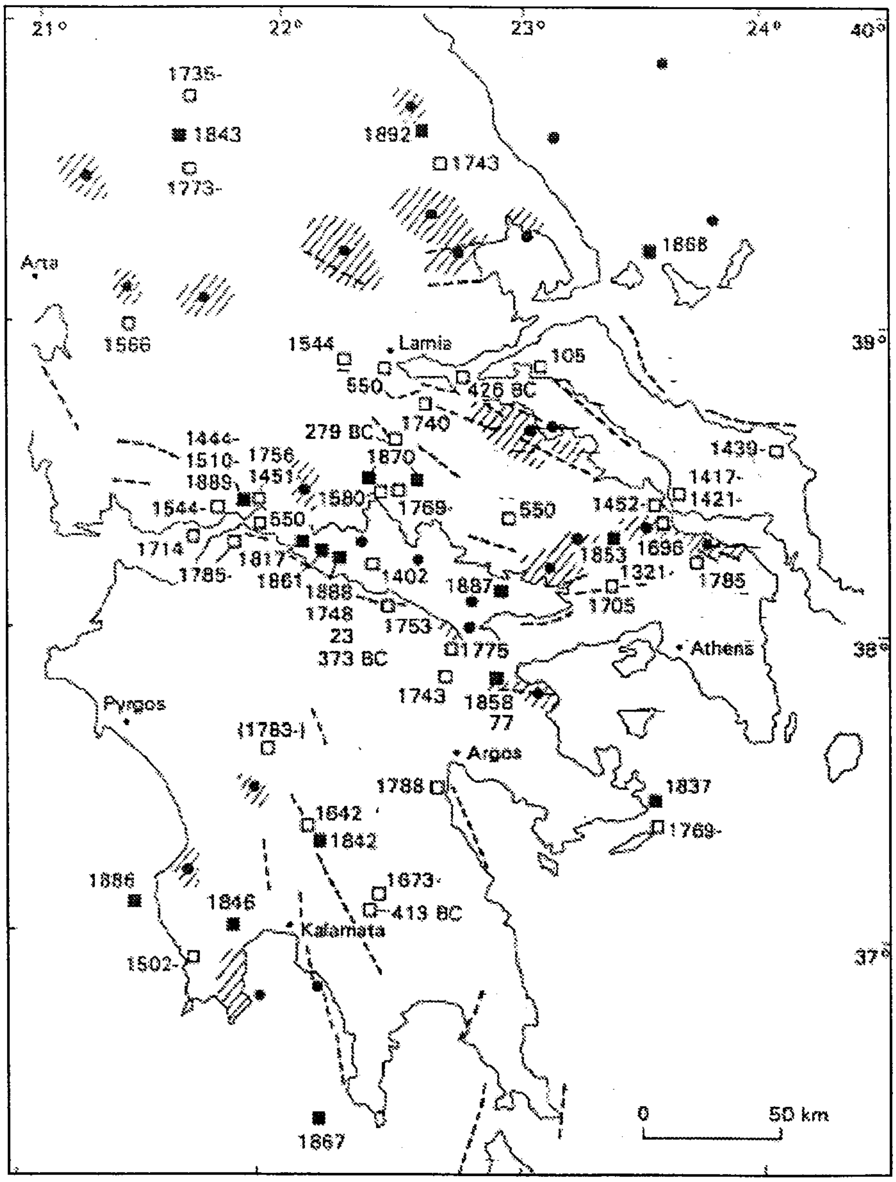

Figure 2. Historical seismicity near Athens (after Ambraseys (1994)).

Table 1 and are shown here in Figure 4b. Figure 5 shows an example of the seismic recordings of the two horizontal components of the broad band sensors of an M_L = 4.4 aftershock as recorded by the GI-NOA broad band network (event No. 9 in Table 1). As one can see from the recordings of the stations PRK, VLS and VAM there are short disruptions in the telemetry communication causing short data

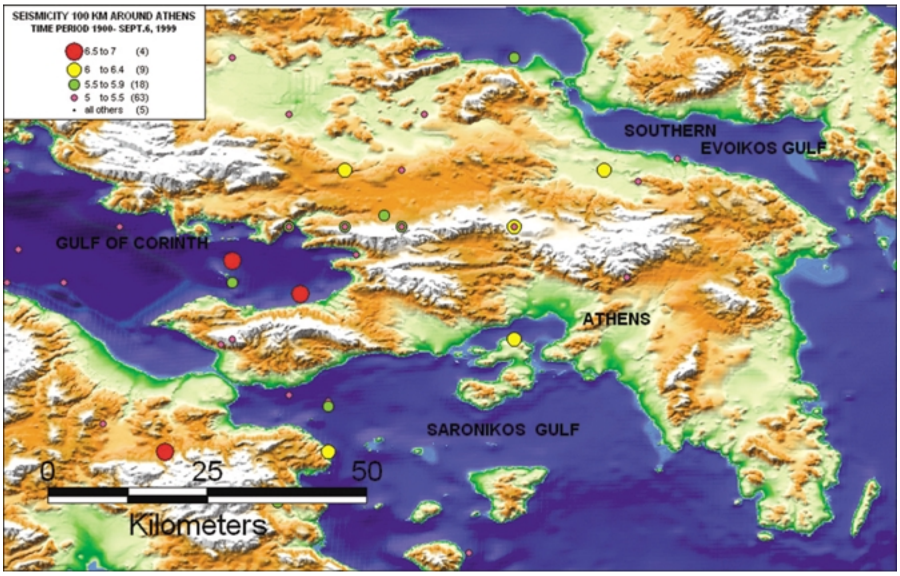

Figure 3. Earthquakes with $M_S > 5$ for the period 1990–6 September 1999.

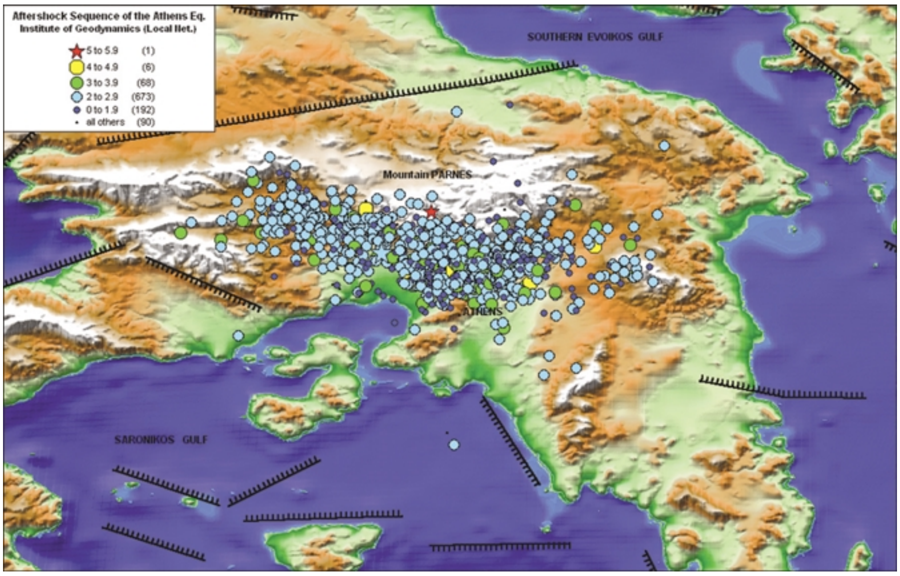

Figure 4a. Main shock and aftershock distribution of the Athens earthquake. Red and blue stars indicate preliminary and relocated epicenter for the main shock. Numbers in brackets indicate number of eartrhquakes for the specific magnitude range.

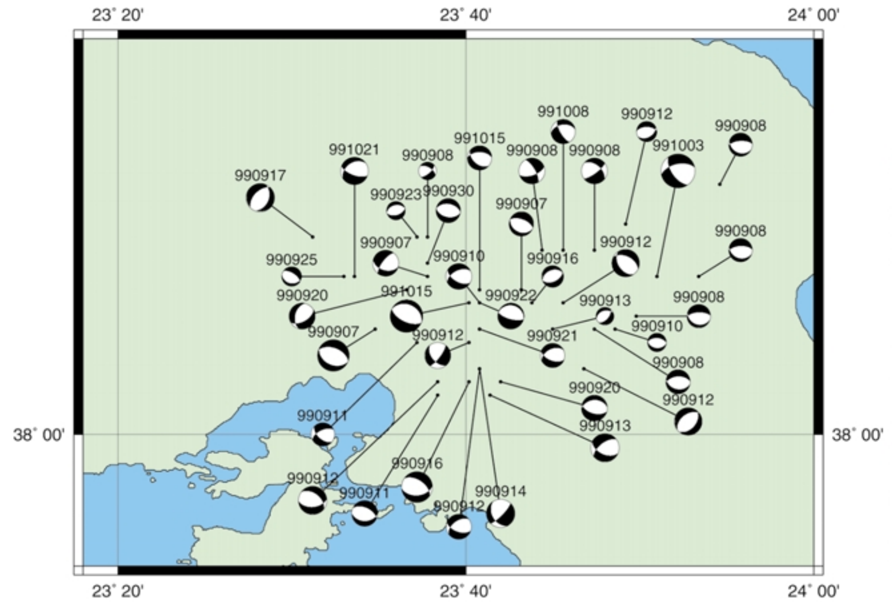

Figure 4b. Focal mechanisms of the main shock and 38 aftershocks after Papadopoulos *et al.* (2000).

disruptions and for this reason in our analysis we were very cautious to choose high quality waveforms for the spectral analysis procedure.

Source parameter determination from spectral analysis of P or S wave data has been the focus of many studies and good examples include the works of Keilis-Borok (1959), Hanks and Wyss (1972), Thatcher and Hanks (1973) and for the Greek area the recent work of Chouliaras and Stavrakakis (1997) summarises the results.

The characteristics of the source for a seismic event are determined from the two parameters of the S wave log-displacement spectra. These parameters are the long period spectral level Ω_0, and the spectral corner frequency F_C (Aki and Richards, 1980).

The analysis procedure used in this study employs the PITSA signal processing toolbox (Scherbaum and Johnston, 1993) and it involves spectral analysis of selected time windows of the S-wave (depending on the $S-P$ arrival time window of the individual trace). In doing this we proceeded to rotate the E-W and N-S recordings which were corrected for the appropriate instrument response, appropriately into radial and tranverse components.

The discrete Fourier spectrum (DTF) is modelled by a Brune source spectrum (Brune, 1970, 1971) and an attenuation operator using a Marquardt-Levenberg non linear inversion technique (Press *et al.*, 1988). As to the noise estimate required for the Chi-square minimization, this is obtained from a single noise window prior to

Table I. List of earthquakes used in this study together with their epicentral coordinates (°N, °E), and local magnitudes (M_L), from the GI-NOA monthly bulletin.

Event No.	Date	Time (G.M.T)	Lat. (°N)	Long. (°E)	M_L
1	7 September 1999	11 56 50.5	38.08	23.58	5.4
2	7 September 1999	13 05 48.5	38.14	23.61	4.1
3	7 September 1999	13 20 3.7	38.17	23.67	3.5
4	7 September 1999	14 43 8.8	38.21	23.72	3.5
5	7 September 1999	15 35 33.3	38.01	23.48	3.9
6	7 September 1999	15 42 52.3	38.07	23.45	3.5
7	7 September 1999	17 19 21.1	38.17	23.61	3.8
8	7 September 1999	20 32 26.7	38.17	23.55	4.1
9	7 September 1999	20 44 55.0	38.19	23.72	4.4
10	8 September 1999	03 21 31.7	38.19	23.71	3.7
11	8 September 1999	03 35 20.6	38.02	23.55	3.7
12	8 September 1999	05 37 8.6	38.40	23.23	3.5
13	8 September 1999	08 23 8.5	38.24	23.47	3.6
14	8 September 1999	12 55 0.4	38.19	23.64	4.0
15	8 September 1999	13 18 21.3	38.10	23.73	3.7
16	8 September 1999	16 50 37.5	38.28	23.81	3.6
17	8 September 1999	16 54 8.0	38.22	23.70	4.0
18	10 September 1999	14 49 56.7	38.14	23.71	3.7
19	12 September 1999	06 17 41.8	38.24	23.75	3.7

the P-wave arrival, using the same window length and tapering parameters as for the signal window.

The starting model parameters for the inversion are obtained interactively using the spectral fitting tool of the PITSA program by Scherbaum and Johnson (1993). Details of the fitting procedure can be found in Scherbaum (1990).

In this procedure, a whole path Q model with a constant $Q = 200$ was chosen and Ω_0 and F_C were adjusted accordingly in the inversion procedure. The choice of the Q value is based on the mean value found in the study of Hashida *et al.* (1988) and which was also used in a similar study to this one, by Chouliaras and Stavrakakis (1997), in which the results were found to be in good agreement with the results from macroseismic surveys in the epicentral regions of some large events (Kozani and Aigio) as well as in this case for the Athens earthquake (Louvari and Kiratzi, 2000). As it was discussed in the study of Chouliaras and Stavrakakis (1997), there is a tradeoff between Q and F_C (high Q-low F_C, and vice versa), however there is a less pronounced effect of the Q value on the determined seismic moment M_0.

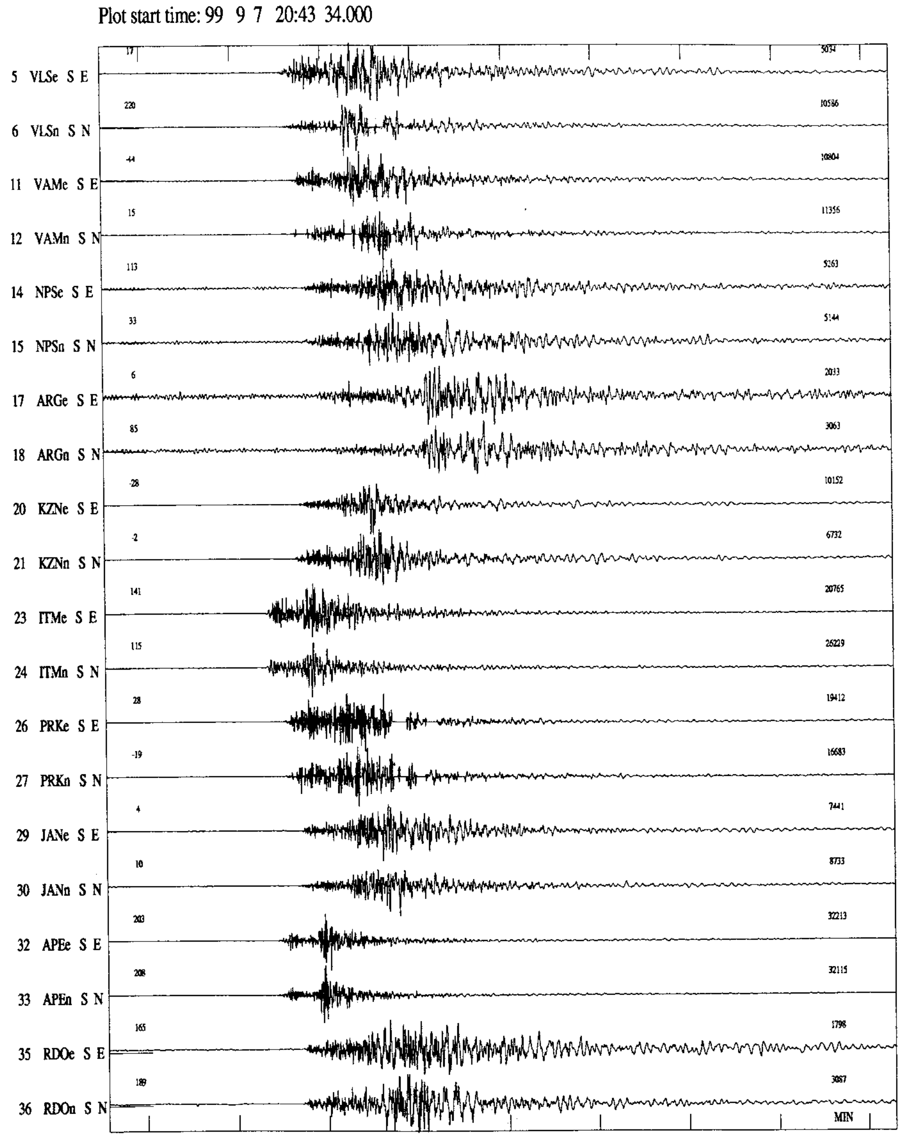

Figure 5. Recording of the two horizontal components (N, E) of an M_L = 4.4 aftershock (event No. 9 in Table 1).

A general feature of all dislocation models is that the long period level Ω_0 is proportional to the seismic moment M_0 and that the corner frequency FC is inversely proportional to the source dimension, r.

Following Keilis-Borok (1959):

$$M_0 = \frac{(4\pi \rho V_S^3 \Omega_0 R)}{(k R_{\Omega\Phi})}, \tag{1}$$

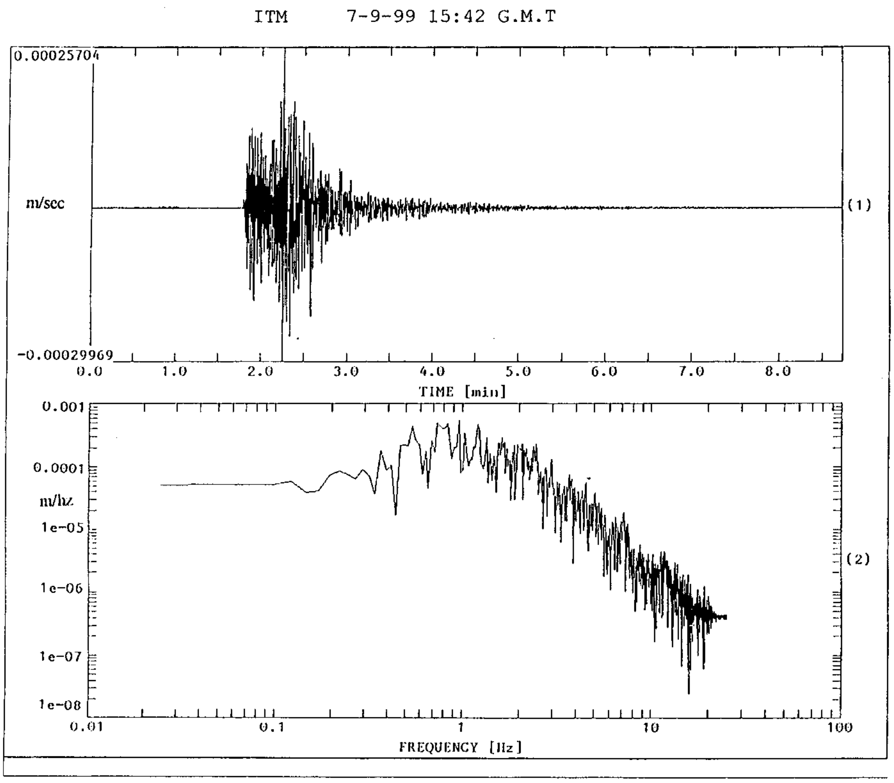

Figure 6a. Recording of the radial component of the rotated E-W and N-S recordings of a ML=3.5 aftershock at the ITM station (event No. 6 in Table 1 and its respective S-wave FFT spectrum.

where ρ = 2.64 g/cm^3 is the density of the medium, R is the hypocentral distance between the source and the receiver, V_S = 3.3 km/sec is the S-wave velocity, k is the free surface operator = 2 and $R_{\Omega\Phi}$ = 0.63 is the average radiation pattern coefficient. Logarithmic weighted averages over all records have been computed (Archuleta *et al.*, 1982) to obtain mean low frequency spectral levels and seismic moments.

The main shock source radius has been computed using the corner frequency FC obtained from the spectral fitting method, also by weighted logarithmic averages (Archuleta *et al.*, 1982) based on the models of Brune (1970, 1971) and Madariaga (1976):

$$\text{Brune model } r_B = \frac{0.37 V_S}{F_C} \tag{2}$$

$$\text{Madariaga model } r_M = \frac{0.21 V_S}{F_C}. \tag{3}$$

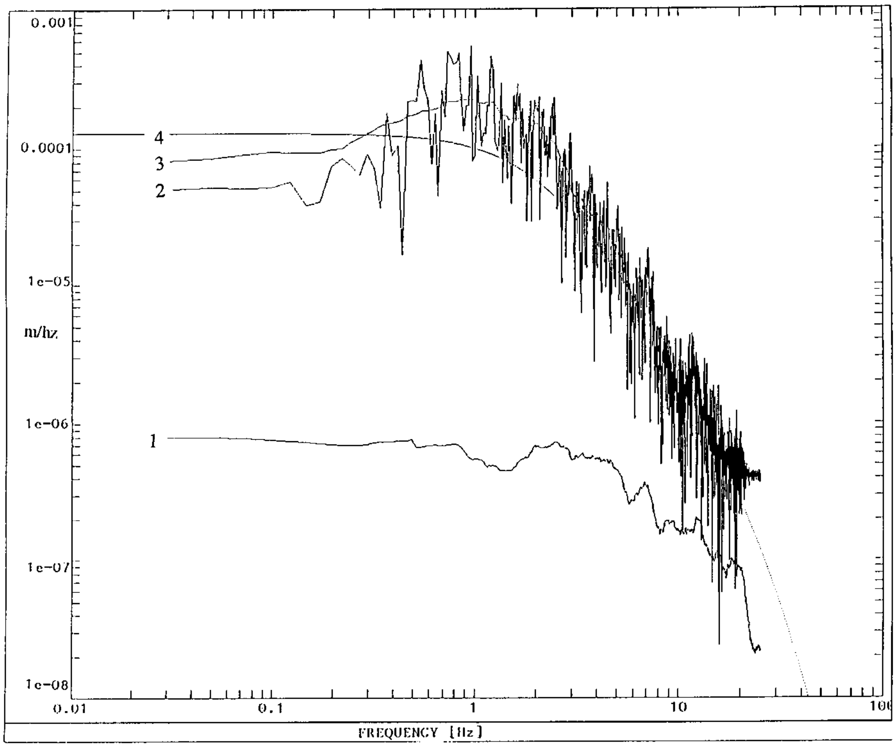

Figure 6b. Spectral fitting result of the radial component from the event shown in Figure 6a. The noise window is trace 1, FFT spectra of the S-wave and it's fitted curve are traces 2 and 3, respectively and the spectral fitting result is trace 4.

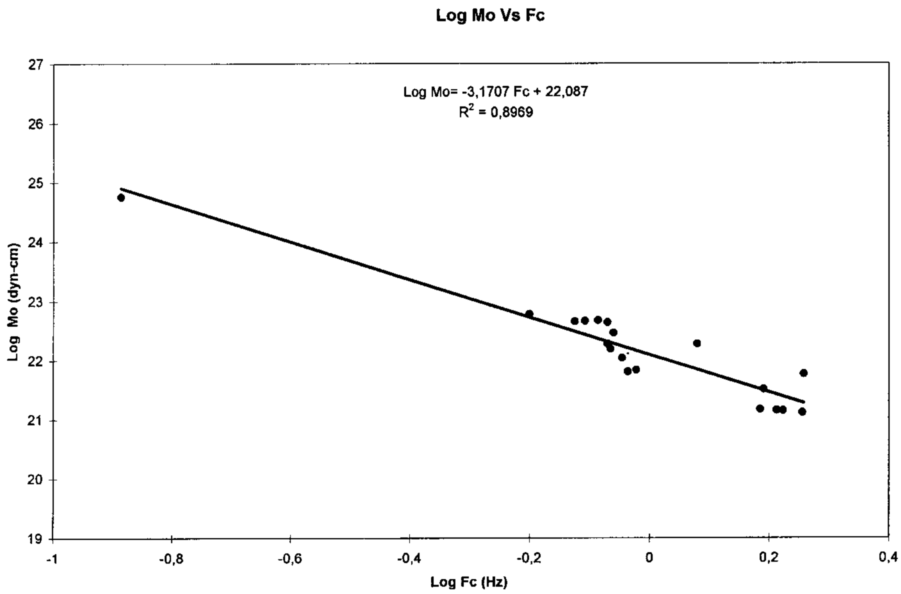

Figure 7. Log M_0 (seismic moment) versus Log F_C (corner frequency for the data set.

Table II. List of the spectral analysis results that concern seismic moment (M_0, in dyn cm), corner frequency (F_C, in Hz), fault radii (r_B, r_M, in Km), stress drops ($\Delta\sigma_B$, $\Delta\sigma_M$, in bars) and displacement (U_B, U_M, in cm). Subscripts B and M refer to the Brune and the Madariaga models, respectively.

	M_L	M_0 (dyn cm)	F_C (Hz)	r_B (km)	r_M (km)	$\Delta\sigma_B$ (bars)	$\Delta\sigma_M$ (bars)	U_B (cm)	U_M (cm)
1	5.4	5.66E+24	0.13	9.39	5.33	3.01	16.44	6.81	21.14
2	4.1	4.33E+22	0.85	1.44	0.82	6.43	35.16	2.23	6.92
3	3.5	1.47E+21	1.53	0.80	0.45	1.27	6.96	0.25	0.76
4	3.5	1.29E+21	1.80	0.68	0.39	1.82	9.95	0.30	0.92
5	3.9	1.88E+22	1.20	1.02	0.58	7.85	42.95	1.93	5.98
6	3.5	1.38E+21	1.67	0.73	0.41	1.55	8.50	0.27	0.85
7	3.8	1.08E+22	0.90	1.36	0.77	1.90	10.41	0.62	1.93
8	4.1	4.51E+22	0.75	1.63	0.92	4.60	25.15	1.81	5.61
9	4.4	5.97E+22	0.63	1.94	1.10	3.61	19.74	1.69	5.24
10	3.7	6.79E+21	0.95	1.29	0.73	1.41	7.70	0.44	1.35
11	3.7	1.89E+22	0.85	1.44	0.82	2.81	15.35	0.97	3.02
12	3.5	1.40E+21	1.63	0.75	0.43	1.47	8.02	0.26	0.82
13	3.6	5.74E+21	1.81	0.67	0.38	8.23	45.00	1.34	4.16
14	4.0	4.58E+22	0.78	1.57	0.89	5.25	28.73	1.98	6.16
15	3.7	2.87E+22	0.87	1.40	0.80	4.57	24.99	1.55	4.80
16	3.6	3.21E+21	1.55	0.79	0.45	2.89	15.80	0.55	1.70
17	4.0	4.70E+22	0.82	1.49	0.85	6.26	34.26	2.25	6.99
18	3.7	1.55E+22	0.86	1.42	0.81	2.38	13.03	0.82	2.53
19	3.7	6.33E+21	0.92	1.33	0.75	1.19	6.52	0.38	1.18

Stress drop ($\Delta\sigma$) and average displacement on the fault plane ($\langle u \rangle$) has been computed from the mean values of seismic moments and source radii of the S wave spectra according to: (Keilis-Borok, 1959; Brune, 1968).

$$\Delta\sigma = \frac{0.44 M_0}{r^3} \tag{4}$$

$$\langle u \rangle = \frac{M_0}{\pi \mu r^2}, \tag{5}$$

where $\mu = 3 \times 10^{10}$ N m^{-2} is the shear modulus.

3. Results and Discussion

Figure 6a shows an example of the rotated radial component component of the 20 sec sensor for a $M_L = 3.5$ aftershock (event 6 in Table 1) that occurred a few hours

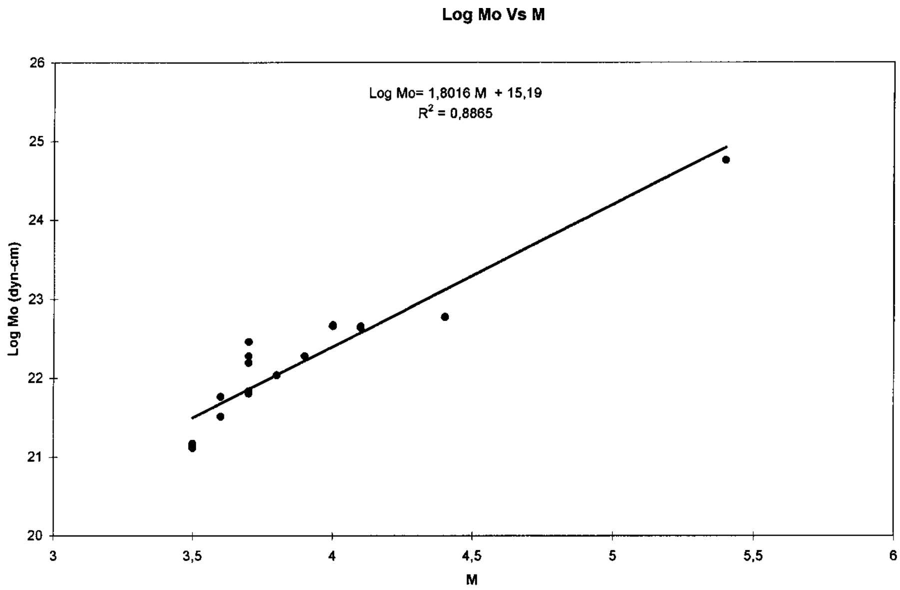

Figure 8. Log seismic moment M_0 versus Local Magnitude M_L for the data set.

after the main shock, recorded by the ITM seismic station, together with the FFT displacement spectrum of the S wave, whereby one is called upon to use an eyeball method to determine the long period level(Ω_0) and the corner frequency(F_C).

For comparison purposes, Figure 6b shows the displacement spectrum of the same radial component and the spectral fitting inversion technique which gives an unbiased estimate of the corner frequency (F_C) and the long period level (Ω_0).

Table 2 lists the results from the spectral fitting inversion method that concern the determination of seismic moment and corner frequency, as well as stress drop and displacement using the models of Brune and Madariaga, for the main shock and the 18 largest aftershocks. In comparing the results for the M_L = 5.4 main shock to other independant results and observations we note the following:

(i) The determined seismic moment of 5.66×10^{24} dyn-cm is comparable to those published by other agencies (Harvard USGS, as well as to the recent results of Louvari and Kiratzi (2000).

(ii) The determined fault radius according to Brune's model is r_B = 9.39 km. This is a reasonable result when compared to the aftershock distribution and to macroseismic evidence (Papadopoulos *et al.*, 2000; Tselentis and Zahradnik, 2000; Pavlides, 1999, 2000) while Madariaga's model with r_M = 5.33 km seems to give lower bounds for the source size.

(iii) The low stress drop of the main shock may be another characteristic of earthquakes in Greece that were identified as complex multiple events by Stavrakakis *et al.* (1986, 1987) and Chouliaras and Stavrakakis (1997) and for the Athens earthquake by Tselentis and Zahradnik (2000).

(iv) The determined displacement according to the Brune model is U_b = 6.81 cm, and this is close to the empirical relations of Papazachos (1994) and other field observations (Pavlides, 1999, 2000), while Madariaga's model appears to give upper bounds for the displacement of this particular event.

The results of this study, concerning scaling relations between seismic moment and the corner frequency and seismic moment and local magnitude are shown in Figures 7 and 8, respectively. The determined relations are:

$$\text{Log } M_0 = -3.17 \text{ Log } F_C + 22.09 \tag{6}$$

and

$$\text{Log } M_0 = 1.80 M_L + 15.2. \tag{7}$$

When comparing the two relations of this study with those from previous investigations, as summarised in Chouliaras and Stavrakakis (1997), we see that they are in good agreement. The present results, even though from a limited data sample give reasonable source parameters for the investigated events and this is promising for relevant studies that concern Greece.

References

Aki, K. and Richards, P. G.: 1980, *Quantitative Seismology: Theory and Methods*, Freeman, San Fransisco, CA.

Ambraseys, N.: 1994, Material for the investigation of the seismicity of central Greece, in Albini and Moroni (eds), *Historical Investigation of the Seismicity of European Earthquakes*, Vol. 2, pp. 1–10.

Archuletta, R. J., Granswick, E., Mueller, C., and Spudich, P.: 1982, Source parameters of the 1980 Mammoth Lakes, California, earthquake sequence, *J. Geophys. Res.* **87**, 4595–4607.

Brune, J. N.: 1968, Seismic moment, seismicity and rate of slip along major fault zones, *J. Geophys. Res.* **73**, 777–794.

Brune, J. N.: 1970, Tectonic stress and the spectra of seismic shear waves from earthquakes, *J. Geophys. Res.* **75**, 4997–5009.

Brune, J. N.: 1971, Correction, *J. Geophys. Res.* **76**, 5002.

Chouliaras, G. and Stavrakakis, G. N.: 1997. Seismic source parameters from a new dial-up seismological network in Greece, *Pure Appl. Geophys.* **150**, 91–111.

Hanks, T. C. and Wyss, M.: 1972, 'The use of body wave spectra in the determination of seismic source parameters, *Bull. Seism. Soc. Am.* **62**, 561–589.

Hashidal, T., Stavrakakis, G., and Shimazaki, K.: 1988, Three-dimensional seismic attenuation structure beneath the Aegean region and it's tectonic implication, *Tectonophysics* **145**, 43–54.

Keilis-Borok, V. I.: 1959, On the estimation of the displacement in an earthquake source and of source dimensions, *Ann. Geof.* **12**, 205–214.

Louvari, E. and Kiratzi, A.: 2000, Source parameters of the 7 September 1999 Athens earthquake based on teleseismic data, *Journal of the Balkan Geophysical Society*, in press.

Madariaga, R.: 1976, Dynamics of an expanding circular fault, *Bull. Seism. Soc. Am.* **66**, 636–666.

Makropoulos, K., Drakopoulos, J., and Latousakis, J.: 1989, A revised and extended earthquake catalog for Greece since 1900, *Geophys. J. Int.* **98**, 391–394.

Papadopoulos, G. A., Drakatos, G., Papanastassiou, D., Kalogeras, and Stavrakakis, G. N.: 2000, Preliminary results about the Catastrophic Earthquake of 7 September 1999 in Athens, Greece, *Seism. Res. Lett.* **71**, 318–329.

Papazachos, B. C.: 1994, Seismology in Greece, *Europ. Seism. Com. Proceedings of the XXIV Gen. Ass.*, Vol. 1, 19–24 September 1994, Athens, pp. 39–57.

Pavlides, S. B., Papadopoulos, G. A., and Ganas, A.: 1999 The 7 September 1999 unexpected earthquake of Athens: Preliminary results on the seismotectonic environment. Presented at the *1st Conference on the Advances on Natural Hazards Mitigation*, 3–4 November, Athens, Greece. Published on pp. 80–85 in Programme reports.

Pavlides, S. B., Papadopoulos, G. A., and Ganas, A.: 2000, Seismic hazard in urban areas: The 7 September 1999 Athens earthquake case study, in K. Takada and H. Goto (eds), *Proceedings of the Hokudan Int. Symp. and School on Active Faulting: Active Fault Research for the New Millenium*, 17–26 January, 2000, Okumura, pp. 367–370.

Press, W. H., Flanerry, B. P., Teukolsky, S. A., and Vetterling, W. T.: 1988, *Numerical Recipes in C*, Cambridge University Press, New York.

Scherbaum, F.: 1990. Combined inversion for the three-dimensional Q structure and source parameters using microearthquake spectra, *J. Geophys. Res.* **95**, 12423–12438.

Scherbaum, F. and Johnston, J.: 1993, PITSA, IASPEI Software library, Vol. 5.

Stavrakakis, G. N., Drakopoulos, J., and Makropoulos, K.: 1986, A rupture model for the Corinth earthquake sequence. Earthquake Prognostics, *Proc. 2nd International Seminar*, 24–27 June, Berlin, pp. 129–153.

Stavrakakis, G., Tselentis, G. A., and Drakopoulos, J.: 1987, Iterative deconvolution of Teleseismic P-waves from the Thessaloniki (Northern Greece) earthquake of 20 June 1978, *Pure Appl. Geophys.* **124**, 1039–1050.

Stavrakakis, G. N., Drakatos, G., Papadopoulos, G. A., and Papanastasiou, D.: 1999, Characteristics of the aftershock sequence of the Athens earthquake of 7 September 1999, based on a local seismographic array. Presented at the *1st Conference on the Advances on Natural Hazards Mitigation*, 3–4 November, Athens, Greece. Published on p. 65 in Programme abstracts.

Thatcher, W. and Hanks, T. C.: 1973. Source parameters of southern California earthquakes, *J. Geophys. Res.* **78**, 8547–8576.

Tselentis, G. A. and Zahradnik, J.: 2000, Aftershock monitoring of the Athens earthquake of 7 September 1999, *Seism. Res. Lett.* **71**, 330–337.